LETTER Communicated by Peter König

Extracting Oscillations: Neuronal Coincidence Detection with Noisy Periodic Spike Input

Richard Kempter
Physik-Department der TU München, D-85747 Garching bei München, Germany

Wulfram Gerstner
Swiss Federal Institute of Technology, Center of Neuromimetic Systems, EPFL-DI, CH-1015 Lausanne, Switzerland

J. Leo van Hemmen
Physik-Department der TU München, D-85747 Garching bei München, Germany

Hermann Wagner
RWTH Aachen, Institut für Biologie II, D-52074 Aachen, Germany

How does a neuron vary its mean output firing rate if the input changes from random to oscillatory coherent but noisy activity? What are the critical parameters of the neuronal dynamics and input statistics? To answer these questions, we investigate the coincidence-detection properties of an integrate-and-fire neuron. We derive an expression indicating how coincidence detection depends on neuronal parameters. Specifically, we show how coincidence detection depends on the shape of the postsynaptic response function, the number of synapses, and the input statistics, and we demonstrate that there is an optimal threshold. Our considerations can be used to predict from neuronal parameters whether and to what extent a neuron can act as a coincidence detector and thus can convert a temporal code into a rate code.

1 Introduction

Synchronized or coherent oscillatory activity of a population of neurons is thought to be a vital feature of temporal coding in the brain. Oscillations have been observed in the visual cortex (Eckhorn et al., 1988; Gray & Singer, 1989), the sensorimotor cortex (Murthy & Fetz, 1992), the hippocampus (Burgess, Recce, & O'Keefe, 1994), and the olfactory system (Freeman, 1975; Davis & Eichenbaum, 1991; Wehr & Laurent, 1996). Coherent firing of neurons might be used for solving the problems of feature linking and pattern segmentation (von der Malsburg & Schneider, 1986; Eckhorn et al.,

1988; Wang, Buhmann, & von der Malsburg, 1990; Ritz, Gerstner, Fuentes, & van Hemmen, 1994; Ritz, Gerstner, & van Hemmen, 1994) and could also support attentional mechanisms (Murthy & Fetz, 1992).

Another prominent example where coherent or phase-locked activity of neurons is known to be important is the early auditory processing in mammals, birds, and reptiles (Carr, 1992, 1993). Spikes are found to be phase locked to external acoustic stimuli with frequencies up to 8 kHz in the barn owl (Köppl, 1997). In the barn owl and various other animals, the relative timing of spikes is used to transmit information about the azimuthal position of a sound source. In performing this task, the degree of synchrony of two groups of neurons is read out and transformed into a firing rate pattern, which can then be used for further processes and to control motor units. The essential step of translating a temporal code into a rate code is performed by neurons that work as coincidence detectors.

Similarly, if neural coding in the cortex is based on oscillatory activity, then oscillations should lead to behavioral actions. Motor output requires a mean level of activity in motor efferents of the order of, say, a hundred milliseconds. But then somewhere in the brain, there must be a neural "unit" that transforms the temporally coded oscillatory activity into a rate-coded mean activity that is suitable for motor output. We do not want to speculate here what this "unit" looks like. It might be composed of an array of neurons, but it is also possible that single neurons perform this transformation.

Here we focus on the question of whether the task of transforming a spike code into a rate code can be done by a single neuron. The issue of how neurons read out the temporal structure of the input and how they transform this structure into a firing rate pattern has been addressed by several authors and is attracting an increasing amount of interest. König, Engel, & Singer (1996) have argued that the main prerequisite for coincidence detectors is that the mean interspike interval is long compared to the integration time that neurons need to sum synaptic potentials effectively. The importance of the effective (membrane) time constant of neurons has also been emphasized by Softky (1994). In addition, Abeles (1982) has shown that the value of the spike threshold and the number of synapses are relevant parameters as well.

Some general principles have already been outlined, but a mathematical derivation of conditions under which neurons can act as coincidence detectors is still not available. In this article, we will substantiate the statements we have already made and show explicitly the dependence of the precision of neuronal coincidence detection on the shape of the postsynaptic potential, the input statistics, and the voltage threshold at which an action potential is generated. Specifically, we tackle the question of whether and to what extent a neuron that receives periodically modulated input can detect the degree of synchrony and convert a time-coded signal into a rate-coded one.

2 Methods

This section specifies the input and briefly reviews the neuron model.

2.1 Temporal Coding of the Input. We consider a single neuron that receives stochastic input spike trains through N independent channels. Input spikes are generated stochastically and arrive at a synapse with a time-dependent T-periodic rate $\lambda^{\text{in}}(t) = \lambda^{\text{in}}(t+T) \geq 0$. The probability of having a spike in the interval $[t, t+\Delta t)$ is $\lambda^{\text{in}}(t)\Delta t$ as $\Delta t \to 0$. In this way we obtain a nonstationary or *inhomogeneous* Poisson process (cf., e.g., Tuckwell, 1988, Sec. 10.8) where input spikes are more or less phase locked to a T-periodic stimulus. According to the definition of Theunissen and Miller (1995), this kind of input is a temporal code. The average number of spikes that arrive during one period at a synapse will be called p. The time-averaged mean input rate is $\bar{\lambda}^{\text{in}} := 1/T \int_{t_0}^{t_0+T} dt' \, \lambda^{\text{in}}(t')$ and equals p/T.

To parameterize the input, we take the function

$$\lambda^{\text{in}}(t) := p \sum_{m=-\infty}^{\infty} G_\sigma(t - mT), \tag{2.1}$$

where $G_\sigma(.)$ denotes a normalized gaussian distribution with zero mean and standard deviation $\sigma > 0$. In Figure 1 we present a few examples of spike trains generated by the time-dependent rate in equation 2.1.

We assume that the neuron under consideration receives input from $N \gg 1$ presynaptic terminals. At each input terminal, spikes arrive independently of the other terminals and with a probability density given by equation 2.1. We note that equation 2.1 is an idealization of biological spike trains because there is no refractoriness.

The degree of synchrony of the input is parameterized by the jitter $\sigma \in [0, \infty)$, the standard deviation of the gaussian distribution. In the case $\sigma = 0$, the input spikes arrive perfectly phase locked and occur only at the times $t_m = mT$ with integer m, and the number of spikes arriving at time t_m has a Poissonian distribution with parameter p. Instead of σ, we often consider another measure of synchrony, the so-called *vector strength* r^{in} (Goldberg & Brown, 1969). This measure of synchrony can be defined as the amplitude of the first Fourier component of the periodic rate in equation 2.1 divided by the Fourier component of order zero. For the input (see equation 2.1) we find

$$r^{\text{in}} = \exp\left[-\frac{1}{2}\left(\frac{2\pi}{T}\right)^2 \sigma^2\right]. \tag{2.2}$$

By construction, we have $0 \leq r^{\text{in}} \leq 1$.

Many neuron models start from a gain function where the mean output firing rate increases with increasing mean input rate. This is certainly cor-

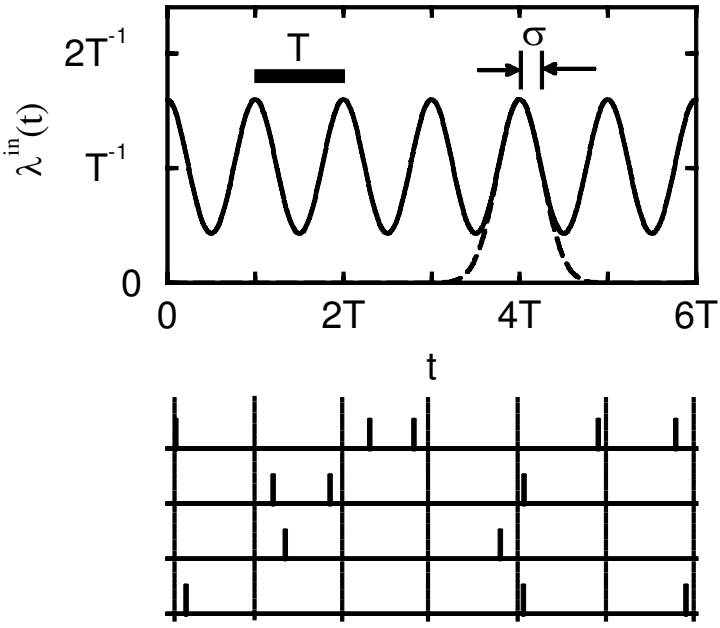

Figure 1: Input spikes are phase locked with period T (horizontal bar) and temporal jitter σ. The upper part of the figure shows the time-dependent rate $\lambda^{\text{in}}(t)$ (solid line) given in equation 2.1 of a single input channel with parameters $p = 1$ and $\sigma = T/4$, the width of the underlying gaussian (dashed line). In the lower part of the figure, we present four samples of spike trains (vertical bars) generated by a Poisson process with the time-dependent rate specified above. The times $t = mT$ with integer m where the rate $\lambda^{\text{in}}(t)$ has its maxima are indicated by vertical dotted lines.

rect for most biological neurons. For integrate-and-fire (I&F) neurons, this property has been studied by Stemmler (1996). In this article, we go at least one step further. We vary the input under the constraint of a *constant* mean input rate, $\bar{\lambda}^{\text{in}} = \text{const}$. The assumption of a constant mean input is not a limitation of our approach but a simplification we make here in order to illustrate our main point. We want to show that even with a constant mean input rate, the mean output rate $\bar{\lambda}^{\text{out}}$ varies as a function of the temporal structure of the input, parameterized, for example, by r^{in}. In other words, the neuron can "read out" a temporal code. This property is essential for coincidence detection.

2.2 Neuron Model and Spike Processing. We describe our neuron as an I&F unit with membrane potential u. The neuron fires if $u(t)$ approaches the threshold ϑ from below. This defines a firing time t^n with integer n. After an output spike, which need not be described explicitly, the membrane potential is reset to 0. Between two firing events, the membrane voltage changes according to the linear differential equation,

$$\frac{\mathrm{d}}{\mathrm{d}t}u(t) = -\frac{1}{\tau_m}u(t) + i(t), \tag{2.3}$$

where i is the total input current and $\tau_m > 0$ the membrane time constant. The input is due to presynaptic activity. The spike arrival times at a given synapse j are labeled by t_j^f where $f = 1, 2, \ldots$ is a running spike index. We assume that there are many synapses $1 \le j \le N$ with $N \gg 1$.

Each presynaptic spike evokes a small postsynaptic current (PSC) that decays exponentially with time constant $\tau_s > 0$. All synapses are equal in the sense that the incoming spikes evoke PSCs of identical shape and amplitude. The total input of the neuron is then taken to be

$$i(t) = \frac{1}{\tau_s}\sum_{j=1}^{N}\sum_f \exp\left(-\frac{t - t_j^f}{\tau_s}\right)\theta(t - t_j^f), \tag{2.4}$$

where $\theta(.)$ denotes the Heaviside step function with $\theta(s) = 0$ for $s \le 0$ and $\theta(s) = 1$ for $s > 0$. We substitute equation 2.4 in 2.3 and integrate. This yields the membrane potential at the hillock,

$$u(t) = \sum_j \left[\sum_f \epsilon(t - t_j^f)\right] + \sum_n \eta(t - t^n). \tag{2.5}$$

The first term on the right in equation 2.5,

$$\epsilon(s) = \frac{\tau_m}{\tau_m - \tau_s}\left[\exp\left(-\frac{s}{\tau_m}\right) - \exp\left(-\frac{s}{\tau_s}\right)\right]\theta(s), \tag{2.6}$$

describes the typical time course of an excitatory postsynaptic potential (EPSP). If $\tau_s = \tau_m$, we have instead of equation 2.6 the so-called alpha function, $\epsilon(s) = (s/\tau_m)\cdot \exp(-s/\tau_m)\,\theta(s)$. The argument below does *not* depend on the precise form of ϵ. The second contribution to equation 2.5,

$$\eta(s) = -\vartheta \exp\left(-\frac{s}{\tau_m}\right)\theta(s), \tag{2.7}$$

accounts for the reset of the membrane potential after each output spike and incorporates neuronal refractoriness.

3 Analysis of Coincidence Detection

We are going to examine the coincidence detection properties of our model neuron. To study the dependence of the output firing rate on the temporal structure of the input and to answer the question of how this is influenced by neuronal parameters, we use the I&F model and the temporally coded spike input already introduced. Qualitative considerations, useful definitions, and illustrating simulations are presented in section 3.1. They explain the gist of why, and how, coincidence detection works. We then return to a mathematical treatment in section 3.2 and finish with some examples in section 3.3.

3.1 The Quality of a Coincidence Detector. We now explain how the ability of a neuron to act as a coincidence detector depends on the leakiness of the integrator (section 3.1.1), the threshold ϑ (section 3.1.2), the time constants τ_m and τ_s (section 3.1.3), and the number N of synapses as well as the mean input rate $\bar{\lambda}^{\text{in}}$ (section 3.1.4).

3.1.1 Leaky or Nonleaky Integrator? The most important parameter of the neuron model is the membrane time constant τ_m. If we take the limit $\tau_m \to \infty$, we are left with a simple nonleaky integrator (cf. equation 2.3). In this case, the mean output rate can be calculated explicitly. Integrating equation 2.3 from the nth output spike at t^n to the next one at t^{n+1} we obtain $\vartheta = \int_{t^n}^{t^{n+1}} \mathrm{d}t\, i(t)$. A summation over M spikes yields

$$\vartheta = \frac{t^{n+M} - t^n}{M} N \bar{\lambda}^{\text{in}} + \frac{1}{M} \int_{t^n}^{t^{n+M}} \mathrm{d}t\, [i(t) - N \bar{\lambda}^{\text{in}}], \tag{3.1}$$

where we have separated the right-hand side into a first term that represents the contribution of the mean input current $N \bar{\lambda}^{\text{in}}$ and a second term that is the fluctuation around the mean. In order to calculate the *mean* output rate $\bar{\lambda}^{\text{out}}$, we have to consider the limit $M \to \infty$. We introduce the mean output rate by defining $\bar{\lambda}^{\text{out}} := \lim_{M\to\infty} M/(t^{n+M} - t^n)$. As $M \to \infty$, the contribution from the second term in the right-hand side of equation 3.1 vanishes, and we are left with $\bar{\lambda}^{\text{out}} = N\bar{\lambda}^{\text{in}}/\vartheta$. The mean output rate is independent of the explicit form of the time-dependent input rate $\lambda^{\text{in}}(t)$, especially r^{in}, which is demonstrated graphically by Figure 2a.

Hence we must have a finite τ_m and thus a leaky integrator, if we want to end up with a coincidence detector, whose rate varies with r^{in}. But what is meant by a "finite" τ_m? The answer depends on the value of the threshold ϑ.

3.1.2 Voltage Threshold. We address the problem of how to adjust the threshold so that an I&F neuron can be used as a coincidence detector. Let

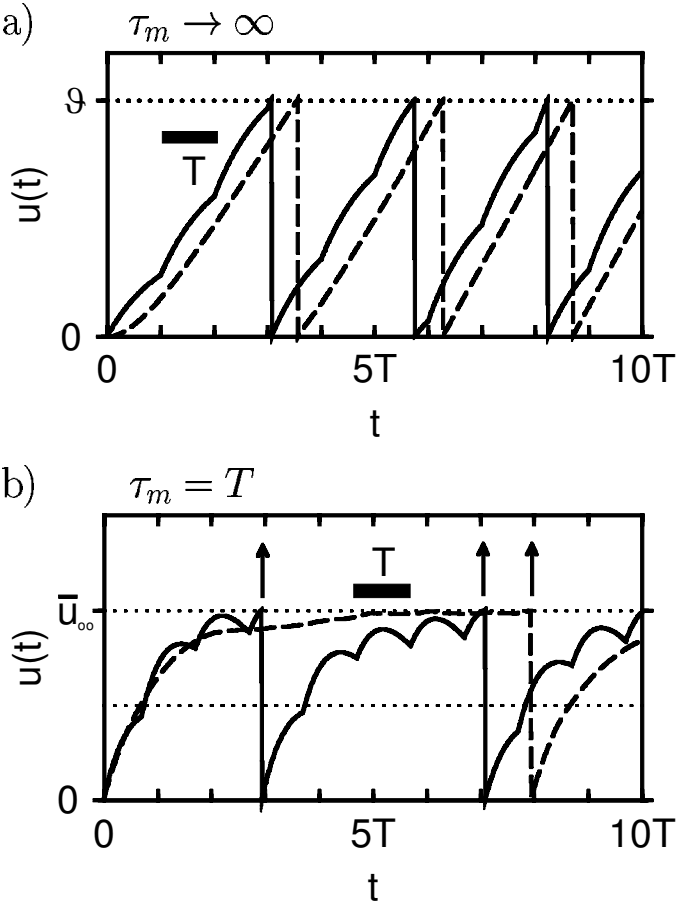

Figure 2: Membrane potential u of an I&F neuron as a function of time t. The neuron receives input from 400 synapses with noise parameter $p = 0.5$ and vector strength $r^{\text{in}} = 1$ (perfectly phase-locked input: solid lines) and $r^{\text{in}} = 0$ (completely random input: dashed lines); cf. eq. 2.1. There is a spike at $t = 0$. The time constant of the synaptic input current is $\tau_s = T$. (a) For an infinitely large membrane time constant τ_m, the intervals between output spikes are nearly independent from the vector strength in the input. Such a neuron is a "bad" coincidence detector. (b) For a finite membrane time constant (here: $\tau_m = T$), the mean interval between output spikes does depend on the vector strength in the input, if the threshold is chosen appropriately. For a threshold $\vartheta = \bar{u}_\infty/2$ (lower dotted line), the first spike would have occurred, nearly independently of the input vector strength r^{in}, somewhere near $t = T$, whereas for a threshold $\vartheta = \bar{u}_\infty$ (upper dotted line) the time to the first spike depends strongly on r^{in}. For $r^{\text{in}} = 1$, the first spike appears near $t = 3\,T$ (left arrow) and a second spike near $t = 7\,T$ (middle arrow). For $r^{\text{in}} = 0$ an output spike occurs at $t = 8\,T$ (right arrow).

us assume for the moment that the firing threshold is very high (formally, $\vartheta \to \infty$), and let us focus on the temporal behavior of the membrane voltage $u(t)$ with some input current i. The membrane potential cannot reach the threshold so that there is neither an output spike nor a reset to baseline, and the membrane voltage fluctuates around the *mean voltage* $\bar{u}_\infty = N\bar{\lambda}^{\text{in}}\tau_m$; see Figure 2b. (The voltage $\bar{u}_\infty$ equals $u(t)$ as $t \to \infty$, provided the total input current is equal to its mean value $i = N\bar{\lambda}^{\text{in}}$.) We now lower the threshold so that the neuron occasionally emits a spike. The coincidence-detection properties of this neuron depend on the location of the threshold ϑ relative to $\bar{u}_\infty$.

We analyze the dependence of the output firing rate on the threshold and the input vector strength r^{in}. As shown in Figure 3a, the mean output firing rate $\bar{\lambda}^{\text{out}}$ is rather insensitive to the input vector strength r^{in} for $\vartheta < \bar{u}_\infty$. We therefore get a poorly performing coincidence detector. In contrast, a threshold $\vartheta > \bar{u}_\infty$ leads to a large variation of the mean output firing rate as a function of the input vector strength r^{in}. Consequently we seem to obtain a better coincidence detector.

The underlying mechanism of this improvement is illustrated by Figure 2b, where the trajectory of the membrane voltage $u(t)$, after a reset at time $t = 0$, is shown for two cases: random and phase-locked input. Let us imagine a threshold ϑ well below $\bar{u}_\infty$, say, at $\bar{u}_\infty/2$. In this case, the next spike following the one at $t = 0$ is triggered after a short time interval, the length of which depends only marginally on the degree of synchrony in the input. We are close to the regime of a nonleaky integrator. Formally, this can be seen from eq. 2.3. Between two firings, the membrane potential always stays below threshold, $u(t) < \vartheta$. If the average current is much larger than ϑ/τ_m, then the first term in the right-hand side of equation 2.3 can be neglected, and we do have a nonleaky neuron. In contrast, let us consider the case $\vartheta > \bar{u}_\infty$. The threshold ϑ can be reached only if the fluctuations of $u(t)$ are large enough. The fluctuations consist of a statistic contribution, due to spike input (shot noise), and periodic oscillations, due to phase-locked (coherent) input. The key observation is that with increasing synchrony in the input, the periodic oscillations get larger and therefore the output firing rate increases. In order to quantify this effect, we introduce a new parameter.

Definition 1. *The ratio of the mean output firing rate* $\bar{\lambda}^{\text{out}}$ *for coherent input with vector strength* $r^{\text{in}} > 0$ *to the rate for completely random input with vanishing vector strength is called the coherence gain* E.

$$E(r^{\text{in}}) := \frac{\bar{\lambda}^{\text{out}}(r^{\text{in}})}{\bar{\lambda}^{\text{out}}(0)}, \text{ with } E(r^{\text{in}}) \geq 1. \tag{3.2}$$

A coherence gain $E(r^{\text{in}}) \approx 1$ means that the I&F neuron does not operate as a coincidence detector, whereas $E(r^{\text{in}}) \gg 1$ hints at good coincidence detection.

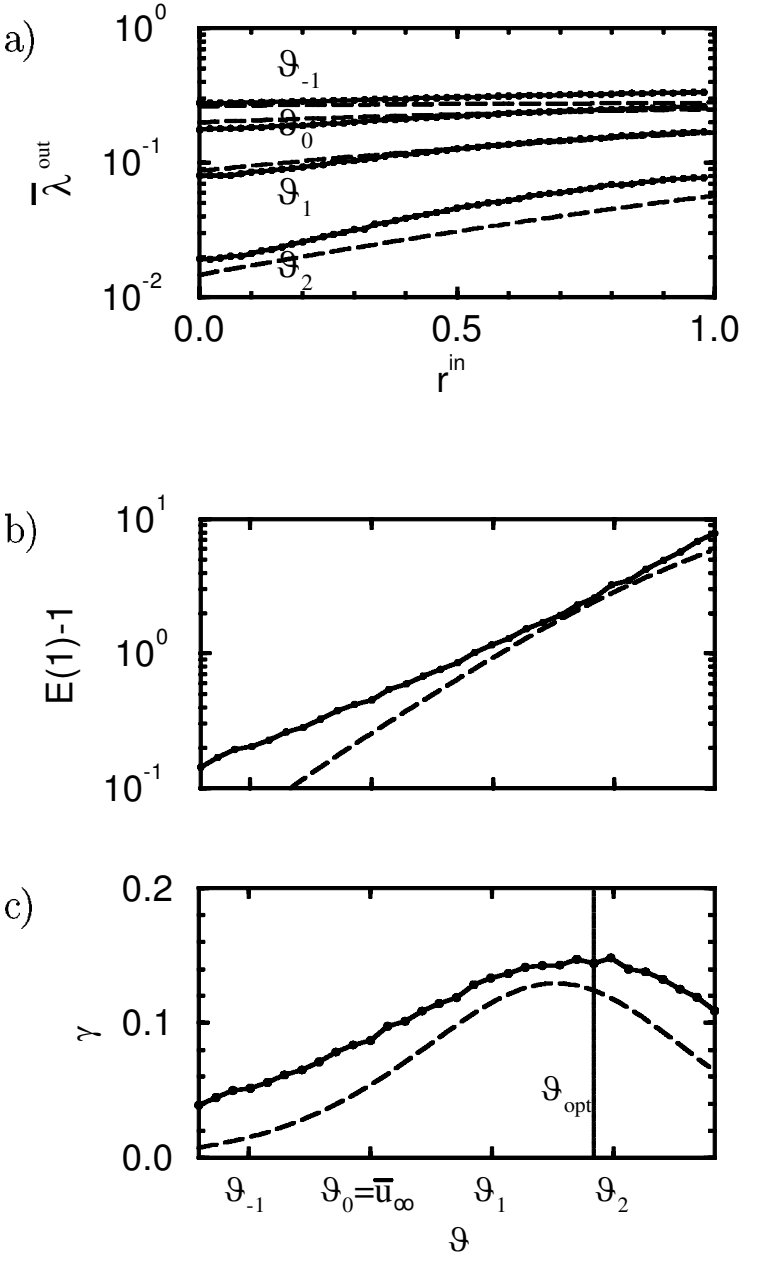
a)
10^0
10^{-1}
10^{-2}
ϑ_{-1}
ϑ_0
ϑ_1
ϑ_2
$\bar{\lambda}^{out}$
0.0
0.5
1.0
r^{in}
b)
10^1
10^0
10^{-1}
E(1)-1
c)
0.2
0.1
0.0
γ
ϑ_{opt}
ϑ_{-1}
$\vartheta_0=\bar{u}_\infty$
ϑ_1
ϑ_2
ϑ

With the above definition of the coherence gain, the four graphs in Figure 3a can be summarized by Figure 3b, where the dependence of $E(r^{\rm in})$ on the threshold is shown for the special case $r^{\rm in} = 1$. The coherence gain $E(1)$ increases with increasing threshold ϑ. From Figure 3b also $E(r^{\rm in})$ for any desired $r^{\rm in}$ can be estimated. Since in first approximation $\bar{\lambda}^{\rm out}$ depends linearly on $r^{\rm in}$, we can use the approximations

$$\bar{\lambda}^{\rm out}(r^{\rm in}) \approx \bar{\lambda}^{\rm out}(0) + r^{\rm in}\,\left[\bar{\lambda}^{\rm out}(1) - \bar{\lambda}^{\rm out}(0)\right] \tag{3.3}$$

and

$$E(r^{\rm in}) \approx 1 + r^{\rm in}\,[E(1) - 1]\,. \tag{3.4}$$

Equation 3.4 tells us that $E(r^{\rm in})$ increases with increasing input vector strength $r^{\rm in}$. Furthermore, $E(r^{\rm in})$ inherits from $E(1)$ the property that it increases with ϑ.

The measure $E(r^{\rm in})$ is useful but not sufficient for characterizing the performance of a coincidence detector because the output of a coincidence detector must convey a signal concerning the nature of the input (coherent or not coherent) in a *finite* amount of time. Neurons with $E(1) \gg 1$ but with a very low mean output rate are basically useless as coincidence detectors.

Figure 3: *Facing page.* Coincidence-detection properties depend on the value of the spiking threshold. We show numerical results (solid lines) and approximations (dashed lines) based on equation 3.21 with $\tau^{\rm dec} = 3/2\ \tau_m$, $\tau^{\rm ref} = 2\ \tau_m$, and ρ determined from equation 3.15 with $A\sqrt{\tau} = \sqrt{\tau_m/2}$. (a) Mean output firing rate $\bar{\lambda}^{\rm out}$ (in units of spikes per period T) as a function of the input vector strength $r^{\rm in}$ for four different values of the threshold ($\vartheta_{-1} = \bar{u}_\infty - \Delta u^{\rm stoch}$, $\vartheta_0 = \bar{u}_\infty$, $\vartheta_1 = \bar{u}_\infty + \Delta u^{\rm stoch}$, $\vartheta_2 = \bar{u}_\infty + 2\Delta u^{\rm stoch}$). The mean voltage is $\bar{u}_\infty = 200$ (as in Figure 2b) and $\Delta u^{\rm stoch} = 10/\sqrt{2}$; cf. equation 3.9. For large ϑ (e.g., ϑ_2) the output rate varies by an order of magnitude if the temporal coherence of the input increases from $r^{\rm in} = 0$ to $r^{\rm in} = 1$. On the other hand, for $\vartheta = \vartheta_{-1}$ the rate $\bar{\lambda}^{\rm out}$ hardly depends on the temporal structure of the input. With $r^{\rm in}$ fixed, the rate $\bar{\lambda}^{\rm out}$ increases with decreasing ϑ in all cases. (b) $E(1) - 1$ is plotted against the threshold ϑ. The coherence gain E is defined in equation 3.2. For the fits in b and c we have $\rho = 0.70$ (for $r^{\rm in} = 1$) in equation 3.21. (c) The parameter γ (in units of $T^{-1/2}I^{1/2}$) that indicates the quality of a coincidence detector shows a maximum at $\vartheta_{\rm opt}$, which is above the mean voltage $\bar{u}_\infty = \vartheta_0$. The value of $\vartheta_{\rm opt}$ is the optimal choice for the threshold of this coincidence detector. In practical situations, it is immaterial, though, whether we take $\vartheta_{\rm opt}$ or, for example, ϑ_1. That is, the choice of the threshold is not critical. Points have been obtained through a combination of equation 3.6 and data from a and b. Simulation parameters in a, b, and c: $\tau_m = \tau_s = T$, $Np = 200$. Data points have been obtained by measuring time intervals that were needed to produce 10^4 output spikes.

This is the case, for example, for leaky I&F units with a voltage threshold well above $\bar{u}_\infty$ (cf. Figure 3a). In this regime the mean output rate is very low. If there is (even for $r^{\text{in}} = 1$) hardly any output spike in a certain time interval, then decisions about the neuron's input can be made only with great error. The other extreme case is a high mean output rate, which implies a threshold well below $\bar{u}_\infty$. In this regime $E(1)$ is low; we are in the regime of a *nonleaky* integrator where neurons are not able to perform a coincidence detection either (cf. Figure 2a). Between the above two limits is an intermediate regime with an *optimal* threshold for coincidence detection. It is "optimal" in the sense that both the spike rate and the coherence gain are high.

The reason that we need a high spike rate is that the number n of output spikes in a finite interval I, from which the rate has to be estimated, is a random quantity. This is because of the noisy input. Here we assume that n is Poisson distributed, an approximation that is very good if spiking is driven by the variance of the neuron's input (Troyer & Miller, 1997). For two different input vector strengths, for example, $r^{\text{in}} = 0$ and $r^{\text{in}} = \hat{r}^{\text{in}} > 0$, we have two different distributions $P(r^{\text{in}})$. The task is to distinguish the two cases based on a single measurement of the number of output spikes in I. We therefore need a number n' as a decision boundary. If $n \geq n'$, then we classify the input to have $r^{\text{in}} = \hat{r}^{\text{in}} > 0$; if $n < n'$, then we classify $r^{\text{in}} = 0$. Clearly the probability for the correct decision depends on n'. In general, the optimal choice for the decision boundary n'_{opt} is the point where the two spike distributions $P(r^{\text{in}} = 0)$ and $P(r^{\text{in}} = \hat{r}^{\text{in}})$ cross (see, e.g., Duda & Hart, 1973).

In order to be able to distinguish reliably the two alternatives, the two respective distributions should not overlap too much. The error increases with decreasing "distance" between them. The distance is a helpful quantity that measures the probability of error or the discriminability between the two possibilities. The *quality factor* for coincidence detection is defined as follows:

Definition 2. *Let the number n of output spikes of a neuron in an interval of length I be Poisson distributed with parameter* $\bar{n}(r^{\text{in}}) = \bar{\lambda}^{\text{out}}(r^{\text{in}})I$, *where* $\bar{\lambda}^{\text{out}}(r^{\text{in}})$ *is the mean output firing rate given an input vector strength* r^{in}. *The normalized distance between the distribution for random input with vanishing vector strength and the distribution for coherent input with some* $r^{\text{in}} > 0$ *is defined to be the quality factor* γ *for coincidence detection. It is obtained by dividing the difference of the distributions' mean values by the sum of their standard deviations,*

$$\gamma := \frac{\bar{n}(r^{\text{in}}) - \bar{n}(0)}{\sqrt{\bar{n}(r^{\text{in}})} + \sqrt{\bar{n}(0)}} = \sqrt{\bar{n}(r^{\text{in}})} - \sqrt{\bar{n}(0)}. \tag{3.5}$$

Using the definition of the coherence gain E in equation 3.2, we obtain

from equation 3.5

$$\gamma = \sqrt{I\,\bar{\lambda}^{\text{out}}(0)}\,\left(\sqrt{E(r^{\text{in}})} - 1\right). \tag{3.6}$$

Equation 3.6 shows how the quality factor γ increases with increasing I, $\bar{\lambda}^{\text{out}}(0)$, and $E(r^{\text{in}})$. It is important to realize that $\bar{\lambda}^{\text{out}}(0)$ and $E(r^{\text{in}})$ are *not* independent variables.

Stemmler (1996) has related a quantity similar to γ to more sophisticated signal-detection quantities such as the "mutual information between the spike counts and the presence or absence of the periodic input" and the "probability of correct detection in the discrimination between the two alternatives," both of which can be expanded in powers of γ. We do not calculate these quantities here as a function of γ. To classify the quality of coincidence detection, γ itself suffices.

In Figure 3c we have plotted γ as a function of the threshold ϑ. This graph clearly shows that there is an *optimal* choice for the threshold ϑ_{opt} that maximizes γ. The quality factor γ as a function of the threshold ϑ generally exhibits a maximum. We argue that $\gamma(\vartheta)$ approaches zero for $\vartheta \to 0$ and also for $\vartheta \to \infty$. Thus, there must be at least one maximum in between. The case $\vartheta \to 0$ corresponds to an infinitely high membrane time constant. This means that the neuron is effectively a nonleaky integrator. For this kind of integrator, the mean output rate does not depend on the input structure. Thus, $E = 1$ and $\gamma(\vartheta) \to 0$ as $\vartheta \to 0$ (cf. equation 3.6). In the case $\vartheta \to \infty$, we argue that $\bar{n}(r^{\text{in}}) \to 0$ for $\vartheta \to \infty$. Since $\bar{n}(r^{\text{in}}) > \bar{n}(0)$ it follows from equation 3.5 that $\gamma \to 0$ as $\vartheta \to \infty$.

The value of the optimal threshold for coincidence detection will be estimated in section 3.2. As we will show there, for a high-quality factor γ, it is not necessary that the threshold be exactly at its optimal value ϑ_{opt}. Since γ depends only weakly on the threshold, the latter is *not* a critical parameter for coincidence detection. In contrast to that, γ varies strongly if we change, say, neuronal time constants.

3.1.3 Neuronal Time Constants. We now point out briefly the dependence of the coherence gain E in equation 3.2, the rate $\bar{\lambda}^{\text{out}}(0)$, and the quality factor γ on the time constants τ_m and τ_s for the special case $\tau_m = \tau_s$. Figures 4a–c show that shorter neuronal time constants yield better coincidence detectors for each of the four different threshold values around ϑ_{opt}. The reason for this effect will be clarified in section 3.2.

3.1.4 Number of Synapses and Mean Input Rate. Since we have N identical and independent synapses receiving, on the average, p spike inputs per period and a linear neuron model (except for the threshold process), the variables N and p enter the problem of coincidence detection only via the product Np, the total number of inputs per period. The quantity Np will be

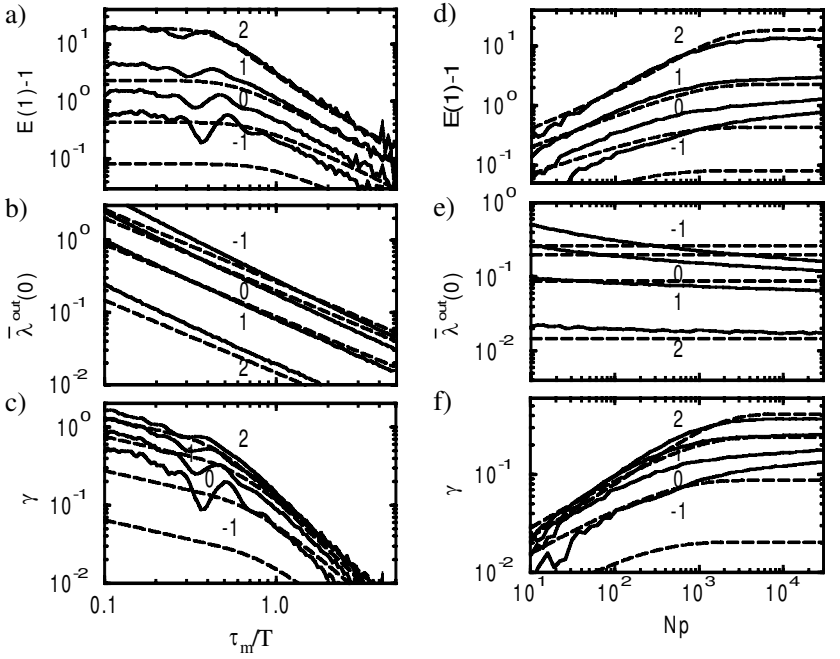

Figure 4: The coherence gain $E(1)$ as defined in equation 3.2 for r^{in}=1, the mean output rate $\bar{\lambda}^{\text{out}}(0)$ for random input in units of spikes per period T, and the quality factor γ in units of $T^{-1/2}\,I^{1/2}$ (cf. equation 3.5) depend on neuronal parameters. Here we illustrate the dependence on the membrane time constant τ_m (left graphs) and the number Np of input spikes per period (right graphs) for four different threshold scenarios in each graph. For the EPSPs we have used equation 2.6 with $\tau_s = \tau_m$. To indicate the position of the threshold, we have assigned the numbers -1, 0, 1, and 2 to each trace (solid lines) that correspond to the indices of the threshold values. We have $\vartheta_{-1} = \bar{u}_\infty - \Delta u^{\text{stoch}}$, $\vartheta_0 = \bar{u}_\infty$, $\vartheta_1 = \bar{u}_\infty + \Delta u^{\text{stoch}}$, and $\vartheta_2 = \bar{u}_\infty + 2\Delta u^{\text{stoch}}$, respectively, where $\bar{u}_\infty = Np\,\tau_m/T$ and $\Delta u^{\text{stoch}} = \sqrt{\bar{u}_\infty}/2$ (cf. also equation 3.9). Fits to the numerical results (dashed lines) are based on equation 3.21 with $\tau^{\text{dec}} = 3/2\,\tau_m$ and $\tau^{\text{ref}} = 2\,\tau_m$. (a–c) The dependence on τ_m is shown. To get a reasonable coincidence detector for $Np = 200$, the time constant τ_m should be at least of the same order of magnitude as T. In fact, this figure has a plain message: The smaller τ_m, the larger $E(1)$, $\bar{\lambda}^{\text{out}}(0)$, and γ . The nonmonotonous part near $\tau_m = 0.35\,T$ is due to resonance effects that occur for widths of EPSPs of the order of T. (d–f) The performance of a coincidence detector also depends on the number Np of input spikes per period. With fixed parameters $\tau_m = \tau_s = T$, the number Np has to exceed 1 substantially so as to get a reasonable coincidence detector. All data points have been obtained by measuring the number of output spikes in a time interval of width $10^5\,T$.

treated as a single degree of freedom. The dependence of $E(1)$, $\bar{\lambda}^{\text{out}}(0)$, and γ on Np is shown in Figures 4d–f. The larger Np, the better is the neuron's performance as a coincidence detector (cf. section 3.2).

To summarize this section, two quantities determine the quality of a coincidence detector neuron: (1) the rate $\bar{\lambda}^{\text{out}}(0)$ and (2) the coherence gain $E(r^{\text{in}})$, which both enter the quality factor γ in equation 3.6. Both quantities depend on neuronal parameters. If, for example, the threshold is increased, then the coherence gain E is enhanced, but at the same time the rate $\bar{\lambda}^{\text{out}}(0)$ is lowered. We note that both the coherence gain $E(r^{\text{in}})$ and $\bar{\lambda}^{\text{out}}(0)$ are, at least in the frame of an I&F model, determined by the neuron's time constants τ_m and τ_s, the period T, the mean number Np of inputs per period, and the threshold ϑ.

3.2 Mathematical Treatment. To transfer the observations from I&F neurons to biological neurons, the quantities τ_m, τ_s, T, and Np have to be determined experimentally. To draw conclusions about the quality of a coincidence detector, knowledge about the spontaneous rate $\bar{\lambda}^{\text{out}}(0)$ and, thus, the threshold ϑ is necessary (cf. equation 3.6). But usually there is no direct access to $E(r^{\text{in}})$ or γ. To close this gap, we present a method of estimating $E(r^{\text{in}})$ and γ from experimentally available parameters.

The mathematical analysis that we present in this subsection is not limited to the I&F model introduced above. We derive our results for a more general class of threshold neurons whose response to an input spike can be described by an EPSP. This class of neuron models has been called the Spike Response Model (SRM) (Gerstner & van Hemmen, 1992, 1994) and can emulate other neuron models, such as the Hodgkin-Huxley model (Kistler, Gerstner, & van Hemmen, 1997).

3.2.1 Signal-to-Noise Ratio Analysis. We perform a signal-to-noise analysis of the membrane potential. Let us assume that the neuron has fired at times $\{t^m; m \leq n\}$. We study the trajectory for $t^n < t < t^{n+1}$ and set

$$u(t) = \bar{u}(t) + \delta u^{\text{stoch}}(t) + \delta u^{\text{per}}(t), \tag{3.7}$$

where $\bar{u}(t) = \sum_m^n \eta(t - t^m) + \bar{u}_\infty$ is the reference trajectory of a neuron that receives a constant input current $N\bar{\lambda}^{\text{in}}$. The membrane potential $u(t)$ follows the trajectory $\bar{u}(t) + \delta u^{\text{per}}(t)$ if it is driven by an input current $N\lambda^{\text{in}}(t)$. Therefore, $\delta u^{\text{stoch}}(t)$ and $\delta u^{\text{per}}(t)$ are the stochastic fluctuations and the periodic oscillations, respectively.

For the signal-to-noise ratio analysis, we de facto presuppose that the noise is gaussian. A normal distribution is the only one that is determined by its first and second moment, which will be used in the following analysis. For a large number N of independent synapses, this is an excellent approximation, as is shown in detail in section A.3.

We have seen before (cf. Figure 2b) that "good" coincidence-detection properties require a threshold ϑ above $\bar{u}_\infty$. In this case, spike generation is driven by the fluctuations, not by the mean trajectory. The magnitude of the stochastic fluctuations is determined by the mean number of input spikes per period and the shape of the EPSP. The amplitude of the periodic fluctuations depends, in addition, on the amount r^{in} of synchrony of the signal. Roughly speaking, the neuron will be able to distinguish between the coherent ($r^{\text{in}} > 0$) and the incoherent case ($r^{\text{in}} = 0$), if the total amount of fluctuation is different in the two cases. The typical amplitude of the fluctuations will be denoted by Δu^{stoch} and Δu^{per}. We define an order parameter

$$\rho := \frac{\Delta u^{\text{per}}(r^{\text{in}})}{\Delta u^{\text{stoch}}(0)}, \tag{3.8}$$

which will be related to the coherence gain E and the quality factor γ. The parameter ρ can be considered as a signal-to-noise ratio, where the signal is given by the periodic modulation and the noise as the stochastic fluctuation of the membrane potential. For $\rho \approx 0$ a low-coherence gain E and quality factor γ is to be expected; for $\rho \gg 1$ there should be a large E and γ. To confirm this conjecture, we relate Δu^{stoch} and Δu^{per} to the parameters of the input and the neuron model.

The calculation of Δu^{stoch} for $r^{\text{in}} = 0$ and Δu^{per} for $r^{\text{in}} \geq 0$ is carried out for a class of typical EPSPs. The only requirement is that EPSPs should, as in equation 2.6, vanish for $s \leq 0$, rise to a maximum, and decay thereafter back to zero (at least exponentially for $s \to \infty$). The amplitude of an EPSP will be called A. The time window preceding any particular point in the neuron's activity pattern during which a variation in the input could have significantly affected the membrane potential is called τ (without a lower index, in contrast to τ_m and τ_s). This is the definition of the integration window of a neuron given by Theunissen and Miller (1995), which can be approximated by the full width at half maximum of the EPSP.

The variance of the stochastic fluctuations is then proportional to the average number of inputs the neuron receives in a time interval τ times the amplitude A of the EPSP (for details see appendix A). For $N\,\bar{\lambda}^{\text{in}}\,\tau \gg 1$ the standard deviation is to good approximation

$$\Delta u^{\text{stoch}}(0) \approx A\sqrt{\frac{N\,\bar{\lambda}^{\text{in}}\,\tau}{2}}\,. \tag{3.9}$$

Using, for example, equation 2.6 in equation A.8, we obtain $A\sqrt{\tau} = \tau_m/\sqrt{\tau_m + \tau_s}$.

To determine the amplitude of periodic oscillations, we average over the Poisson process of the membrane voltage in equation 2.5 and denote the average by angular brackets $\langle . \rangle$. From equation 3.7 we have $\langle u - \bar{u} \rangle(t) =$

$\langle \delta u^{\rm per} \rangle(t)$, since $\langle \delta u^{\rm stoch} \rangle(t) = 0$, and thus

$$\langle \delta u^{\rm per} \rangle(t) = N \int_0^\infty {\rm d}s \left[\lambda^{\rm in}(t-s) - \bar{\lambda}^{\rm in} \right] \epsilon(s). \tag{3.10}$$

The amplitude $\Delta u^{\rm per}$ of the T-periodic oscillations will be estimated by the absolute value of the first Fourier coefficient of $\langle \delta u^{\rm per} \rangle(t)$. The kth Fourier coefficient of a T-periodic function $x(t)$ is defined by

$$\tilde{x}_k := \frac{1}{T} \int_t^{t+T} {\rm d}t'\, x(t')\, \exp(-i\,k\,\omega\,t'), \text{ with } \omega := \frac{2\pi}{T}. \tag{3.11}$$

Now the amplitude of the periodic oscillations can be written as

$$\Delta u^{\rm per} = \left| \left\langle \delta \tilde{u}_1^{\rm per} \right\rangle \right|. \tag{3.12}$$

To calculate the right-hand side of equation 3.12, we also have to introduce the Fourier transform of quadratically integrable functions, for example, of the response kernel ϵ defined in equation 2.6,

$$\tilde{\epsilon}(\omega) := \int_{-\infty}^\infty {\rm d}t'\, \epsilon(t')\, \exp(-i\,\omega\,t'). \tag{3.13}$$

Carrying out the Fourier transform in equation 3.12 and using equation 3.13, we obtain $\Delta u^{\rm per} = N\,|\tilde{\lambda}_1^{\rm in}\,\tilde{\epsilon}(\omega)|$, where $\tilde{\lambda}_1^{\rm in} = p/T\, r^{\rm in} = \bar{\lambda}^{\rm in}\, r^{\rm in}$ is the first Fourier coefficient of $\lambda^{\rm in}$ defined in equation 2.1. The final result for the signal amplitude is then

$$\Delta u^{\rm per} = N\,\bar{\lambda}^{\rm in}\, r^{\rm in}\, |\tilde{\epsilon}(\omega)|, \tag{3.14}$$

where the definition of the vector strength $r^{\rm in}$ in equation 2.2 has been used. The order parameter ρ in equation 3.8 can be rewritten with equations 3.9 and 3.14 in terms of experimentally accessible parameters of the input and neuronal parameters:

$$\rho \approx r^{\rm in} \sqrt{2\,N\,\bar{\lambda}^{\rm in}\,\tau}\, \frac{|\tilde{\epsilon}(\omega)|}{A\,\tau}. \tag{3.15}$$

One has to keep in mind that equation 3.15 contains the signal-to-noise ratio in the membrane potential and concerns only one of two aspects of coincidence detection. The second aspect is related to the mean output firing

rate and, thus, the threshold, which should be chosen appropriately, as we discussed in section 3.1 (see also section 4). The order parameter ρ alone can be used only to derive necessary conditions for coincidence detection. For small ρ, it seems unlikely that a neuron acts as a coincidence detector, but a small ρ could be compensated for by a pool of such neurons (see also sections 3.3 and 4). We think that as a rule of thumb, one can exclude that a neuron is a coincidence detector if $\rho < 0.1$.

Taking advantage of equation 3.15, we now derive an expression for the mean output rate $\bar{\lambda}^{\text{out}}(r^{\text{in}})$ and for γ .

3.2.2 Mean Output Rate. As we stated in the previous section, in the absence of a firing threshold, the neuron's membrane voltage fluctuates around a mean value $\bar{u}_\infty$ with a standard deviation Δu^{stoch}, which is due to noisy input. From appendix A, we also know that, to excellent approximation, the voltage fluctuations are gaussian. Then the probability that at an arbitrary time the membrane voltage u is above ϑ can be estimated by

$$w(\vartheta) = \frac{1}{\sqrt{2\pi}\,\Delta u^{\text{stoch}}} \int_{\vartheta}^{\infty} \mathrm{d}u \, \exp\left[-\frac{(u - \bar{u}_\infty)^2}{2\,(\Delta u^{\text{stoch}})^2} \right], \tag{3.16}$$

which can be rewritten in terms of the error function,

$$w(\vartheta) = \frac{1}{2}\left[1 - \operatorname{erf}\left(\frac{\vartheta - \bar{u}_\infty}{\sqrt{2}\,\Delta u^{\text{stoch}}} \right) \right]. \tag{3.17}$$

If $\vartheta > \bar{u}_\infty$, the average time that a voltage fluctuation stays above ϑ is called τ^{dec}, which is expected to be of the order of the width τ of the integration window. The time τ^{dec} is needed for a decay of any voltage fluctuation. Therefore, the mean time interval between two events $u > \vartheta$ can be approximated by $\tau^{\text{dec}}/w(\vartheta)$.

A neuron's dynamics is such that firing occurs if the membrane voltage reaches the threshold ϑ from below. After firing, there is a refractory period τ^{ref} during which the neuron cannot fire. This prolongs the mean waiting time $\tau^{\text{dec}}/w(\vartheta)$ until the next event $u = \vartheta$ by an amount of τ^{ref}. Taking refractoriness into account, the mean interspike interval τ^{isi} can be approximated by

$$\tau^{\text{isi}} \approx \tau^{\text{dec}}/w(\vartheta) + \tau^{\text{ref}}. \tag{3.18}$$

The mean output rate is $\bar{\lambda}^{\text{out}} = 1/\tau^{\text{isi}}$. Substituting equation 3.17 into 3.18, we obtain the mean output rate for a random input,

$$\bar{\lambda}^{\text{out}}(0) = \left\{ 2\tau^{\text{dec}} \left[1 - \operatorname{erf}\left(\vartheta'/\sqrt{2} \right) \right]^{-1} + \tau^{\text{ref}} \right\}^{-1}. \tag{3.19}$$

Here we have introduced the normalized threshold,

$$\vartheta' = (\vartheta - \bar{u}_\infty)/\Delta u^{\text{stoch}}. \tag{3.20}$$

If the neuron's input has a periodic contribution, then the output rate is increased. We now calculate the rate $\bar{\lambda}^{\text{out}}(r^{\text{in}})$ for arbitrary $r^{\text{in}} \geq 0$. The key assumption is that we are allowed to take the oscillatory input into account through a modified threshold ϑ' only. The periodic contribution enhances the standard deviation of the membrane potential around its mean value. Thus, the threshold is lowered by the normalized amplitude of the periodic oscillations $\rho(r^{\text{in}})$ of the membrane potential (cf. equation 3.8). A generalization of equation 3.19 leads to

$$\bar{\lambda}^{\text{out}}(r^{\text{in}}) \approx \left\{ 2\tau^{\text{dec}} \left[1 - \text{erf}\left(\vartheta' - \rho/\sqrt{2} \right) \right]^{-1} + \tau^{\text{ref}} \right\}^{-1}. \tag{3.21}$$

Since we have an expression for the mean output rate in equation 3.21, we also have an expression for the coherence gain E and the quality factor γ (cf. equations 3.2 and 3.6). In Figure 3 the numerical results for $\bar{\lambda}^{\text{out}}$, E, and γ can be fitted at least within an order of magnitude by using $\tau^{\text{dec}} = 3/2\ \tau_m$ and $\tau^{\text{ref}} = 2\ \tau_m$.

3.2.3 Quality Factor. To arrive at a better understanding of the dependence of the quality factor γ on the normalized threshold ϑ' and the signal-to-noise ratio ρ, we have plotted the result for γ (ϑ') in Figure 5 while taking $\tau^{\text{dec}} = 3/2\ \tau_m$ and $\tau^{\text{ref}} = 2\ \tau_m$ (as in Figures 3 and 4) for different values of ρ. The graphs illustrate that γ varies only weakly as a function of ϑ', if ρ is held constant. The maximum value is, at least for $0 < \rho < 1$, close to $\vartheta' = 1$. This confirms the result of Figure 3c and the conjecture that the optimal threshold lies above the mean voltage by an amount equal to the amplitude of the stochastic fluctuations.

To get a handy expression for γ, we use an approximation of the error function (Ingber, 1982),

$$\frac{1}{2}\left[1 - \text{erf}(x)\right] \approx \frac{1}{1 + \exp\left(4x/\sqrt{\pi}\right)}, \tag{3.22}$$

which is better than 2% for all x. At least for $0 < \rho \ll 1$ we are able to derive a simple expression for γ. Using the definition for γ in equation 3.6 and a linearization in ρ, we obtain

$$\gamma = \rho \sqrt{\frac{2}{\pi} \frac{I}{\tau^{\text{dec}}}} \left[1 + \exp \hat{\vartheta} + \tau^{\text{ref}}/\tau^{\text{dec}} \right]^{-3/2} \exp \hat{\vartheta}, \tag{3.23}$$

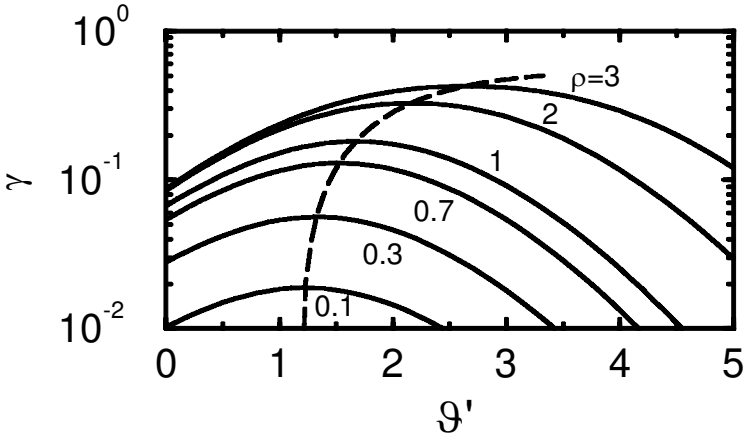

Figure 5: The quality factor γ (in units of $\tau_m^{-1/2} I^{1/2}$) defined in equation 3.6 for the model of $\bar{\lambda}^{\text{out}}$ in equation 3.21 as a function of the dimensionless threshold ϑ' defined in equation 3.20. The quantity γ has been plotted (solid lines) for six different values of ρ, as indicated in the graph. The time constants in equation 3.21 have been chosen to agree with numerical results from simulations of an I&F model when EPSPs are "alpha" functions. Thus, it is reasonable to assume $\tau^{\text{ref}} = 2\,\tau_m$ (cf. equation 2.7) and $\tau^{\text{dec}} = 3/2\,\tau_m$ (see also Figures 3 and 4). For each value of ρ, the quantity γ (ϑ') is a smoothly varying function of ϑ' and shows a single maximum. The dashed line connects the maxima. The value of ϑ' at the maximum is the optimal threshold for coincidence detection. For $\rho < 1$, the optimal threshold is approximately at $\vartheta' = 1$. Since the maxima are broad, the threshold value is *not* critical for coincidence detection.

where we have used $\hat{\vartheta} = 4\,\vartheta'/\sqrt{2\pi}$. For $0 < \rho \ll 1$, the quality factor has a maximum as a function of the threshold at

$$\hat{\vartheta}_{\text{opt}} = \ln\left[2\,(1 + \tau^{\text{ref}}/\tau^{\text{dec}})\right]. \tag{3.24}$$

Substituting $\hat{\vartheta}_{\text{opt}}$ to equation 3.23 and inserting ρ from equation 3.15, we get an upper bound for the quality factor, which is the key result of this article:

$$\gamma \le \gamma_{\text{opt}} = r^{\text{in}} \sqrt{2\,N\,\bar{\lambda}^{\text{in}}\,\tau}\,\frac{|\tilde{\epsilon}(\omega)|}{A\,\tau} \cdot \sqrt{\frac{I}{\tau^{\text{dec}} + \tau^{\text{ref}}}}\,\frac{4}{\sqrt{54\pi}}. \tag{3.25}$$

3.3 Examples. We are using the response kernel $\epsilon(s) = (s/\tau_m)\exp(-s/\tau_m)\cdot\theta(s)$ in equation 2.5. The absolute value of the Fourier transform is $|\tilde{\epsilon}(\omega)| =$

$\tau_m/\left(1+\omega^2\tau_m^2\right)$. From equations 3.15 and A.8 (see also the remark after equation 3.9), we then obtain the signal-to-noise ratio,

$$\rho = \sqrt{N\,\bar{\lambda}^{\rm in}\,\tau_m}\,\frac{2\,r^{\rm in}}{1+\omega^2\tau_m^2}. \tag{3.26}$$

Let us calculate ρ for cortical neurons. Due to background activity, the (effective) membrane time constant for voltages in the neighborhood of the threshold can be as low as 10 ms (Bernander, Douglas, Martin, & Koch, 1991; cf. also Rapp, Yarom, & Segev, 1992). We assume EPSPs as "alpha" functions and $N = 10^4$ synapses firing at $\bar{\lambda}^{\rm in} = 5$ Hz. If the input has a periodic component of 40 Hz ($T = 25$ ms), we calculate from equation 3.26 a value of $\rho = 6.1\,r^{\rm in}$. The vector strength $r^{\rm in}$ can be related to the relative modulation amplitude $A^{\rm rel}$ of almost periodic correlograms by $r^{\rm in} \approx \sqrt{A^{\rm rel}/2}$ (see appendix B), which is a good approximation for small $A^{\rm rel}$. A value of $A^{\rm rel} \approx 0.3$ is reasonable (Gray & Singer, 1989). We find $r^{\rm in} \approx 0.4$, and a signal-to-noise ratio of $\rho \approx 2.4$. Therefore cortical neurons possess all prerequisites necessary for coincidence detection.

As a further application of equation 3.26, we turn to neurons in the *nucleus laminaris* of the barn owl. Model studies have shown that the laminar neurons can indeed act as coincidence detectors (Gerstner, Kempter, van Hemmen, & Wagner, 1996). These neurons have (almost) no dendritic trees. A set of parameters $N = 200$, $\tau_m = \tau_s = 0.1$ ms, $\bar{\lambda}^{\rm in} = 0.5$ kHz, $\bar{\lambda}^{\rm out} = 100$ Hz, and $r^{\rm in} = 0.5$ for $T^{-1} = 5$ kHz is reasonable (Carr & Konishi, 1990; Carr & Boudreau, 1991; Reyes, Rubel, & Spain, 1996). From equation 3.26, we obtain $\rho = 0.29$. This value should be compared to the much better signal-to-noise ratio $\rho \approx 2.4$ that we find for cortical neurons.

We now compare the values of the upper bound of the quality factor $\gamma_{\rm opt}$ in equation 3.25 for the two types of neurons. We take an interval of, say, $I = 100$ ms to get some numerical values that can be interpreted, though the length of I is not important for the comparison. For cortical neurons we assume $\tau^{\rm dec} = 3/2\,\tau_m$ and $\tau^{\rm ref} = 2\,\tau_m$, the parameters used throughout the whole article. From equation 3.25, we then obtain $\gamma_{\rm opt} = 1.2$. For laminar neurons, we also assume $\tau^{\rm dec} = 3/2\,\tau_m$ and $\tau^{\rm ref} = 2\,\tau_m$, whereby $\tau_m = 0.1$ ms, and obtain $\gamma_{\rm opt} = 1.5$. We conclude that both types of neurons have comparable coincidence-detection properties. In laminar neurons, the relatively low number N of synapses is compensated by a high mean input rate $\bar{\lambda}^{\rm in}$ in order to achieve the same performance as cortical neurons. In both examples, the ratio τ_m/T and the input vector strength $r^{\rm in}$ were almost identical.

What does a quality factor of, say, $\gamma = 1.5$ mean? We remind readers of the definition of γ in equation 3.5. The quality factor is a quantity that measures the distance between the spike count distributions for random and coherent input. For $\gamma = 1$, the two distributions are just distinguishable, and for $\gamma \gg 1$ they are well separated. The error probability or, better, the extent

to which random and coherent input can be discriminated can be calculated from γ . The corresponding algorithm is the subject of further investigation.

4 Discussion

This study demonstrates the influence of the parameters of an I&F neuron on the capability of the neuron to work as a coincidence detector for periodically modulated spike input. The dependence on the membrane time constant τ_m has been demonstrated in Figures 2 and 4a–c, the influence of the number of inputs per period Np was treated in Figures 4d–f, and the relation to the threshold ϑ has been shown in Figures 3 and 5. An order parameter ρ for coincidence detection has been defined in equation 3.15 by dividing the amplitude of the periodic oscillations (when the neuron receives phase-locked input) by the amplitude of the stochastic fluctuations of the membrane voltage (when the neuron receives random input). Finally, ρ has been related to the quality factor γ for coincidence detection.

Our reasoning is not limited to I&F neurons. It can be applied directly to neurons whose excitatory synapses have almost equal strengths and evoke similar EPSPs that sum up linearly, at least below the threshold. The extension to a distribution of synaptic strengths and forms of EPSPs is also straightforward. With some additional effort, phase-locked inhibitory inputs could also be incorporated. Our model does not include, though, nonlinear effects in the dendritic tree (Softky, 1994).

The shape of the EPSP plays the most important role for coincidence detection. More precisely, the relevant parameter is the absolute value of the Fourier component of the response kernel ϵ at the frequency of the external stimulus (cf. equation 3.15), which expresses the (low-pass) filtering property of synaptic transmission. Nevertheless, the rule of thumb holds that the briefer the EPSPs, the better are the coincidence-detection properties of the corresponding neuron. The width of the EPSP has to be at least of the same order of magnitude as the minimal temporal structure it should resolve (cf. Figure 4a).

In addition, the number of synapses and their mean activity determine whether a neuron is able to perform coincidence detection. With T-periodically modulated input, our results show that the more input spikes per time, the easier is coincidence detection (cf. Figure 4b). This is due to the fact that the ratio between the signal (= oscillations of membrane voltage) and the noise (= random fluctuations) increases with increasing mean input rate. The contribution of many synapses also enhances coincidence-detection properties, which is extremely important for neurons receiving a large number of inputs, such as cortical pyramidal cells with about 10^4 synapses or cerebellar purkinje cells with approximately $2 \cdot 10^5$ synapses.

One can summarize the influence of the width τ of an EPSP and the number of inputs per time a neuron receives on coincidence detection as follows. The neuron's "memory" extends over an interval τ back in time,

so the neuron cannot "see" earlier input spikes. They have little influence on the membrane potential because the corresponding tails of the EPSPs are small and decay exponentially in time. (For the moment, we neglect refractory effects.) Hence, the number of inputs in the neuron's integration time window of length τ determines the state (the membrane potential) of the neuron. If the number of inputs in this shifting time window shows a significant T-periodic oscillation, then it is in principle possible that the neuron is able to perform coincidence detection. This is a rate-coding scheme where the firing rate has to be measured within an averaging time window. This argument shows that the width of an EPSP, which corresponds to the averaging time window, should be small. If it greatly exceeds one period, then averaging will be of no use at all.

For coincidence detection there is an optimal threshold value, as illustrated by Figures 3c and 5. For optimal coincidence detection, the threshold ϑ has to surpass the mean membrane voltage $\bar{u}_\infty = N\,\bar{\lambda}^{\rm in}\,\tau_m$ of the neuron by an amount equal to the noise amplitude. A higher threshold implies a lower mean output firing rate, which destroys the advantage of a high-coherence-gain E. A lower threshold leads to the regime of a nonleaky integrator, which is not at all suited to coincidence detection. Thus coincidence detection in "real" neurons requires an adaptive mechanism to control the threshold. There are several different possibilities for that. First, we could imagine a control loop that adjusts the threshold in the appropriate regime. This might be difficult to implement but could be achieved, for example, if each spike is followed by a long-lasting hyperpolarizing afterpotential. Alternatively, we could envisage a feedback loop of inhibitory neurons that adjust the mean input. A control of input strength is also possible through synaptic changes (Tsodyks & Markram, 1997; Abbott, Varela, Sen, & Nelson, 1997). Finally, it has been shown in a model study (Gerstner et al., 1996) that potentiation and depression of synaptic weights can balance each other so that the effective input strength is always normalized (see also Markram, Lübke, Frotscher, & Sackmann, 1997). However, the threshold is *not* a critical parameter for coincidence detection, as is illustrated by the *broad* maximum of γ as a function of the threshold in Figures 3c and 5. The threshold also determines the mean firing rate of a neuron. For reasonable firing rates, the quality factor remains of the same order of magnitude as its optimal value $\gamma_{\rm opt}$ (cf. equation3.25).

The existence of an optimal threshold can be related to the phenomenon of stochastic resonance (Wiesenfeld & Moss, 1995) in that in the presence of noise, the detection of weak signals can be enhanced and there is an optimal noise level. It seems unlikely, though, that neurons are able to change the level of noise in their input. A neuron has potentially the chance of adapting its threshold to an optimal value, as we have discussed before. We have shown that the optimal threshold for coincidence detection is, similar to stochastic resonance, always above $\bar{u}_\infty$ by an amount that is of the same order of magnitude as the noise amplitude.

Having the parameter γ at hand, one still has to be careful with rash conclusions about a neuron's task. Let us consider a neuron whose γ is small. One might argue that such a neuron cannot function as a coincidence detector, and this is certainly correct if we consider the neuron as a single unit. But if there is a pool of neurons operating in the same pathway and receiving the same type of input, the output of all these neurons together could provide a secure cue for a decision. Also, the waiting time, which is necessary to make a correct decision with high reliability, can be reduced by using a pool of neurons. That is, the following two counting methods are equivalent: a system can use either the output spike count of a single neuron in an interval I or the number of spikes of L statistically independent, identical neurons operating in the same pathway during a period of time I/L.

Although we have considered the transition from spike to rate coding, the output spikes remain phase locked to a periodic input. This means that the neuronal transmission always retains some of the temporal information, an aspect that we think is important to signal processing in the brain.

Appendix A: Inhomogeneous Poisson Process

In this appendix we define and analyze the inhomogeneous Poisson process. This notion has been touched on by Tuckwell (1988, pp. 218–220) and others (e.g., Ash & Gardner, 1975, pp. 28–29), but neither of them explains the formalism itself or the way of computing expectation values. Since both are used extensively, we do so here, despite the fact that the issue is treated by Snyder and Miller (1991, secs. 2.1–2.3). Our starting assumptions in handling this problem are the same as those of Gnedenko (1968, sec. 51) for the homogeneous (uniform) Poisson process, but the mathematics is different. Neither does our method resemble the Snyder and Miller approach, which starts from the other end, equation A.11. In the context of theoretical neurobiology, an analysis such as this one, focusing on the local behavior of a process, seems to us far more natural. We proceed by evaluating the mean and the variance and finish this appendix by estimating a third moment, which is needed for the Berry-Esseen inequality, that tells us how good a gaussian approximation to a sum of independent random variables is.

A.1 Definitions. Let us suppose that a certain event, in our case a spike, occurs at random instances of time. Let $N(t)$ be the number of occurrences of this event up to time t. We suppose that $N(0) = 0$, that the probability of getting a single event during the interval $[t, t + \Delta t)$ with $\Delta t \to 0$ is

$$\Pr\{N(t + \Delta t) - N(t) = 1\} = \lambda(t)\,\Delta t\,, \qquad \lambda \geq 0\,, \tag{A.1}$$

and that the probability of getting two or more events is $o(\Delta t)$. Finally, the process has independent increments; events in disjoint intervals are

independent. The stochastic process obeying the above conditions is an inhomogeneous Poisson process.

Under conditions on λ to be specified below, there are only finitely many events in a finite interval. Hence, the process lives on a space Ω of monotonically nondecreasing, piecewise constant functions on the positive real axis, having finitely many unit jumps in any finite interval. The expectation value corresponding to this inhomogeneous Poisson process is simply an integral with respect to a probability measure μ on Ω, a function space whose existence is guaranteed by the Kolmogorov extension theorem (Ash, 1972, sec. 4.4.3). A specific realization of the process, a function on the positive real axis, is a "point" ω in Ω. The discrete events corresponding to ω are denoted by $t_f(\omega)$ with f labeling them.

As we have seen in eq. 2.5, spikes generate postsynaptic potentials ϵ. We now compute the average, denoted by angular brackets, of the postsynaptic potentials generated by a specific neuron during the time interval $[t_0, t)$,

$$\left\langle \sum_f \epsilon(t - t_f(\omega)) \right\rangle . \tag{A.2}$$

Here it is understood that $t_f = t_f(\omega)$ depends on the realization ω and $t_0 \le t_f(\omega) < t$. We divide the interval $[t_0, t)$ into L subintervals $[t_l, t_{l+1})$ of length Δt so that at the end $\Delta t \to 0$ and $L \to \infty$ while $L\,\Delta t = t - t_0$. We now evaluate the integral (see equation A.2), exploiting the fact that ϵ is a continuous function.

Let $\#\{t_l \le t_f(\omega) < t_{l+1}\}$ denote the number of events (spikes) occurring at times $t_f(\omega)$ in the interval $[t_l, t_{l+1})$ of length Δt. In the limit $\Delta t \to 0$, the expectation value (see equation A.2) can be written

$$\int_\Omega \mathrm{d}\,\mu(\omega) \left[\sum_l \epsilon(t - t_l)\, \#\{t_l \le t_f(\omega) < t_{l+1}\} \right], \tag{A.3}$$

so that we are left with the Riemann integral,

$$\int_{t_0}^{t} \mathrm{d}\,s\, \lambda(s)\, \epsilon(t - s) . \tag{A.4}$$

We spell out why. The function $\mathbb{1}_{\{\ldots\}}$ is to be the indicator function of the set $\{\ldots\}$ in Ω; that is, $\mathbb{1}_{\{\ldots\}}(\omega) = 1$, if $\omega \in \{\ldots\}$ and it vanishes if ω does not belong to $\{\ldots\}$, so it "indicates" where the set $\{\ldots\}$ lives. With the benefit of hindsight, we single out mutually independent sets in Ω with indicators $\mathbb{1}_{\{t_l \le t_f(\omega) < t_{l+1}\}}$ and write the expectation value (see equation A.2) in the form

$$\int_\Omega \mathrm{d}\,\mu(\omega) \sum_l \mathbb{1}_{\{t_l \le t_f(\omega) < t_{l+1}\}} \epsilon(t - t_l)\, \#\{t_l \le t_f(\omega) < t_{l+1}\} . \tag{A.5}$$

Each indicator function in the sum equals

$$\mathbb{1}_{\{t_l \le t_f(\omega) < t_{l+1}\}} = \mathbb{1}_{\{N(t_{l+1})-N(t_l)=0\}} + \mathbb{1}_{\{N(t_{l+1})-N(t_l)=1\}} + \mathbb{1}_{\{N(t_{l+1})-N(t_l)\ge 2\}}. \tag{A.6}$$

In view of equations A.2 and A.5, we multiply this by $\epsilon(t-t_l)\,\#\{t_l \le t_f(\omega) < t_{l+1}\}$, interchange integration and summation in equation A.5, and integrate with respect to μ. The first term on the right contributes nothing; the second gives $\lambda(t_l)\epsilon(t-t_l)\Delta t$ and thus produces a term in the Riemann sum leading to equation A.4; and the last term can be neglected since it is of order $o(\Delta t)$. The proof of the pudding is that only a single event in the interval $[t_l, t_{l+1})$ counts as $\Delta t \to 0$. Since $\epsilon(t)$ is a function that decreases at least exponentially as fast as $t \to \infty$, there is no harm in taking $t_0 = -\infty$.

A.2 Second Moment and Variance. It is time to compute the second moment,

$$\left\langle [\sum_{t_f < t} \epsilon(t-t_f)]^2 \right\rangle . \tag{A.7}$$

In a similar vein as before, we obtain, in the limit $\Delta t \to 0$,

$$\begin{aligned}
&\left\langle \sum_{t_f, t'_f < t} \epsilon(t-t_f)\epsilon(t-t'_f) \right\rangle \\
&= \int_\Omega \mathrm{d}\,\mu(\omega) \sum_{l,m} \mathbb{1}_{\{t_l \le t_f(\omega) < t_{l+1}\}} \mathbb{1}_{\{t_m \le t'_f(\omega) < t_{m+1}\}} \epsilon(t-t_f(\omega))\epsilon(t-t'_f(\omega)) \\
&= \sum_{l \ne m} [\lambda(t_l)\Delta t\, \lambda(t_m)\Delta t]\, \epsilon(t-t_l)\epsilon(t-t_m) + \\
&\qquad \int_\Omega \mathrm{d}\,\mu(\omega) \sum_l \mathbb{1}^2_{\{t_l \le t_f(\omega) < t_{l+1}\}} \epsilon^2(t-t_l) \\
&= \int_{t_0}^t \int_{t_0}^t \mathrm{d}\,t_1 \mathrm{d}\,t_2\, \lambda(t_1)\lambda(t_2)\epsilon(t-t_1)\epsilon(t-t_2) + \int_{t_0}^t \mathrm{d}\,s\, \lambda(s)\epsilon^2(t-s) \\
&= \left[\int_{t_0}^t \mathrm{d}\,s\, \lambda(s)\epsilon(t-s) \right]^2 + \int_{t_0}^t \mathrm{d}\,s\, \lambda(s)\epsilon^2(t-s).
\end{aligned} \tag{A.8}$$

Hence the variance is the last term on the right in equation A.8. It is a simple exercise to verify that when $\lambda(t) \equiv \lambda$ and $\epsilon(t) \equiv 1$ in equations A.4 and A.8, we regain the mean and variance of the usual Poisson distribution.

We finish the argument by computing the probability of getting k events in the interval $[t_0, t)$. For the usual, homogeneous Poisson process it is

$$\Pr\{N(t) - N(t_0) = k\} = \exp[-\lambda(t-t_0)] \cdot \frac{[\lambda(t-t_0)]^k}{k!} . \tag{A.9}$$

We now break up the interval $[t_0, t)$ into many subintervals $[\tau_l, \tau_{l+1})$ of length Δt and condition with respect to the first, second, ..., arrival. The arrivals come one after the other, and the probability of a specific sequence of events in $[t_1, t_1 + \Delta t)$, $[t_2, t_2 + \Delta t)$, ..., $[t_k, t_k + \Delta t)$ is made up of elementary events such as

$$\begin{aligned}
&\Pr\{\text{First spike in } [t_1, t_1 + \Delta t)\} \\
&\quad = \Pr\{\text{no spike in } [t_0, t_1)\} \Pr\{\text{spike in } [t_1, t_1 + \Delta t)\} \\
&\quad = [1 - \lambda(\tau_1)\Delta t][1 - \lambda(\tau_2)\Delta t] \ldots [1 - \lambda(t_1 - \Delta t)\Delta t]\, \lambda(t_1)\Delta t \\
&\quad = \exp\left[-\int_{t_0}^{t_1} \mathrm{d}\,\tau\, \lambda(\tau)\right] \lambda(t_1)\Delta t. \qquad \text{(A.10)}
\end{aligned}$$

Here we have exploited the independent-increments property and taken the limit $\Delta t \to 0$ to obtain the last equality. Repeating the above argument for the following events, including the no-event tail in $[t_k + \Delta t, t)$, multiplying the probabilities, and summing over all possible realizations, we find

$$\begin{aligned}
&\Pr\{N(t) - N(t_0) = k\} \\
&\quad = \exp\left[-\int_{t_0}^{t} \mathrm{d}\,\tau\, \lambda(\tau)\right] \int_{t_0}^{t} \mathrm{d}\,t_k\, \lambda(t_k) \ldots \int_{t_0}^{t_3} \mathrm{d}\,t_2\, \lambda(t_2) \int_{t_0}^{t_2} \mathrm{d}\,t_1\, \lambda(t_1) \\
&\quad = \exp\left[-\int_{t_0}^{t} \mathrm{d}\,\tau\, \lambda(\tau)\right] \cdot \frac{1}{k!} \left[\int_{t_0}^{t} \mathrm{d}\,s\, \lambda(s)\right]^k. \qquad \text{(A.11)}
\end{aligned}$$

In other words, $N(t) - N(t_0)$ has a Poisson distribution with parameter $\int_{t_0}^{t} \mathrm{d}\,s\, \lambda(s)$. If $\lambda(s) \equiv \lambda$, one regains equation A.9. We now see two things. First, the appropriate condition on λ is that it be locally integrable. Then $\Pr\{N(t) - N(t_0) < \infty\} = 1$ as the sum of equation A.11 over all finite k adds up to one. Furthermore, $N(t) - N(t')$ with $t_0 < t' < t$ has a Poisson distribution with parameter $\int_{t'}^{t} \mathrm{d}\,s\, \lambda(s)$. Second, by rescaling time through $t := \int^t \mathrm{d}\,s\, \lambda(s)$ one obtains (Tuckwell, 1988; Ash & Gardner, 1975) a homogeneous Poisson process with parameter $\lambda = 1$. This also follows more directly from equation A.1. It is of no practical help for understanding neuronal coincidence detection, though. For instance, if we use a spike train generated by an inhomogeneous Poisson process with rate $\lambda(t)$ to drive, such as a leaky I&F neuron, its mean output firing rate does depend on the temporal structure of $\lambda(t)$, as we have argued. This effect cannot be explained by simply rescaling time. Another example is provided by the auditory system, where $\lambda(t)$ is taken to be a periodic function of t, with the period determined by external sound input. The cochlea, however, produces a whole range of frequency inputs, whereas time can be rescaled only once.

A.3 Berry-Esseen Estimate. Equation 2.5 tells us that the neuronal input is a sum of independent, identically distributed random variables corresponding to neighboring neurons j. Neither independence nor a common

distribution is necessary, but both are quite convenient. The point is that, according to the central limit theorem, a sum of N independent random variables[1] has a gaussian distribution as $N \to \infty$. In our case, N is definitely finite, so the question is: How good is the gaussian approximation? The answer is provided by a classical, and remarkable, result of Berry and Esseen (Lamperti, 1966, sec. 15).

We first formulate the Berry-Esseen result. Let $X_1, X_2, \ldots$ be independent with a common distribution having variance σ^2 and finite third moment. Furthermore, let $S_N = \sum_{j=1}^{N}(X_j - \langle X_j \rangle)$ be the total input, the X_j stemming from neighboring neurons j as given by the right-hand side of equation 2.5 with N as the number of synapses, and let Y_σ be a gaussian with mean 0 and variance σ^2. Then there is a constant $(2\pi)^{-1/2} \le C < 0.8$ such that, whatever the distribution of the X_j and whatever x,

$$\left| \Pr\left\{ \frac{S_N}{\sqrt{N}} \le x \right\} - \Pr\{Y_\sigma \le x\} \right| \le \frac{C\langle |X_1 - \langle X_1 \rangle|^3 \rangle}{\sigma^3 \sqrt{N}} . \tag{A.12}$$

In the present case, σ^2 directly follows from equation A.8. Computing $\langle |X_1 - \langle X_1 \rangle|^3 \rangle$ is a bit nasty but it is simpler, and also provides more insight, to estimate the third moment directly by Cauchy-Schwartz so as to get rid of the absolute value,

$$\langle |X_1 - \langle X_1 \rangle|^3 \rangle \le \langle (X_1 - \langle X_1 \rangle)^2 \rangle^{1/2} \langle (X_1 - \langle X_1 \rangle)^4 \rangle^{1/2} . \tag{A.13}$$

The first term on the right equals σ; the second is given by

$$\langle (X_1 - \langle X_1 \rangle)^4 \rangle = \int_{t_0}^{t} \mathrm{d}\, s\, \lambda(s)\, \epsilon^4(t-s) + 3\sigma^4, \tag{A.14}$$

where $\sigma^2 = \int_{t_0}^{t} \mathrm{d}\, s\, \lambda(s) \epsilon^2(t-s)$. Collecting terms, we can estimate the right-hand side of equation A.12, the precision of the gaussian approximation being determined by $1/\sqrt{N}$ as N becomes large.

Appendix B: Cross-Correlograms and Degree of Synchrony

Here we outline the relationship between the relative modulation A^{rel} of cross-correlograms and the underlying degree of synchrony, r^{in}.

A spike input generated by equation 2.1 leads to a periodic cross-correlation function,

$$C(t) \propto \sum_{m=-\infty}^{\infty} G_{\sigma\sqrt{2}}(t - mT). \tag{B.1}$$

[1] This N directly corresponds with the number of synapses that provide the neuronal input. There is no need to confuse it with the stochastic variable $N(t)$ of the previous subsection.

The relative amplitude A^{rel} of C is to be defined below. It is estimated from the Fourier transform of C, which is defined in equation 3.11. The Fourier coefficients of equation B.1 are

$$\tilde{C}_k \propto \exp\left[-(k\,\sigma\,\omega)^2\right] \text{ with } \omega = \frac{2\pi}{T}. \tag{B.2}$$

For $\sigma\,\omega > 1$ the first Fourier component dominates, all higher coefficients can be neglected, and we can approximate equation B.1 by

$$C(t) \approx \tilde{C}_0 + 2\,\tilde{C}_1 \cos(t), \tag{B.3}$$

where $2\,\tilde{C}_1$ is the amplitude of the first-order oscillation. Then A^{rel}, defined as the relative modulation of the cross-correlogram (cf., e.g., König, Engel, & Singer, 1995), is approximated by

$$A^{\text{rel}} \approx \frac{2\,\tilde{C}_1}{\tilde{C}_0}. \tag{B.4}$$

Substituting equation B.2 into B.4, we obtain

$$A^{\text{rel}} \approx 2\,\exp\left[-(\sigma\,\omega)^2\right]. \tag{B.5}$$

Using the definition of the vector strength (see equation 2.2) in B.5 and solving for r^{in}, we find

$$r^{\text{in}} \approx \sqrt{\frac{A^{\text{rel}}}{2}}. \tag{B.6}$$

The restriction $\sigma\,\omega > 1$ corresponds to $r^{\text{in}} < 0.6$ or $A^{\text{rel}} < 0.7$.

The oscillation amplitude of the cross-correlation function $C(t)$ for spike activity as found in various brain areas decays to zero with increasing $|t|$ (cf. Gray & Singer, 1989) because neuronal activity is not strictly periodic. Most of the cross-correlograms can be fitted by using generalized Gabor functions of the form (cf., for example, König et al., 1995)

$$C(t) \propto 1 + A^{\text{rel}} \cos(t)\,\exp\left(-\frac{t^2}{\lambda^2}\right), \tag{B.7}$$

where λ is a time constant. In this case we obtain a measure of the degree of synchrony r^{in} also from equation B.6, which originally was derived for the periodic case only. The transfer of the arguments from the periodic to the nonperiodic case is reasonable if λ is of the order of a few oscillation periods T or longer. For coincidence detection, only correlations within the integration time τ of a neuron are important. For neurons that are able to act as coincidence detectors, τ has to be at least of the order of T, so that reasonable coincidence detectors do not "see" the decay of the correlation function.

Acknowledgments

We thank Julian Eggert and Werner Kistler for stimulating discussions, helpful comments, and a careful reading of the manuscript. We also thank Jack Cowan and Richard Palmer for some useful hints concerning the title. This work has been supported by the Deutsche Forschungsgemeinschaft under grant numbers He 1729/8-1 (RK) and He 1729/2-2, 8-1 (WG).

References

Abbott, L. F., Varela J. A., Sen K., & Nelson S. B. (1997). Synaptic depression and cortical gain control. *Science, 275*, 220–224.

Abeles, M. (1982). Role of the cortical neuron: Integrator or coincidence detector? *Isr. J. Med. Sci., 18*, 83–92.

Ash, R. B. (1972). *Real analysis and probability*. New York: Academic Press.

Ash, R. B., Gardner, M. F. (1975). *Topics in stochastic processes*. New York: Academic Press.

Bernander, Ö., Douglas, R. J., Martin, K. A. C., & Koch C. (1991). Synaptic background activity influences spatiotemporal integration in single pyramidal cells. *Proc. Natl. Acad. Sci. USA, 88*, 11569–11573.

Burgess, N., Recce, M., & O'Keefe, J. (1994). A model of hippocampal function. *Neural Networks, 7*, 1065–1081.

Carr, C. E. (1992). Evolution of the central auditory system in reptiles and birds. In D. B. Webster, R. R. Fay, & A. N. Popper (eds.), *The evolutionary biology of hearing* (pp. 511–543). New York: Springer-Verlag.

Carr, C. E. (1993). Processing of temporal information in the brain. *Ann. Rev. Neurosci., 16*, 223–243.

Carr, C. E., & Boudreau, R. E. (1991). Central projections of auditory nerve fibers in the barn owl. *J. Comp. Neurol., 314*, 306–318.

Carr, C. E., & Konishi, M. (1990). A circuit for detection of interaural time differences in the brain stem of the barn owl. *J. Neurosci., 10*, 3227–3246.

Davis, J. L., & Eichenbaum, H. (Eds.). (1991). *Olfaction: A model system for computational neuroscience*. Cambridge, MA: MIT Press.

Duda, R. O., & Hart, P. E. (1973). *Pattern classification and scene analysis*. New York: Wiley.

Eckhorn, R., Bauer, R., Jordan, W., Brosch, M., Kruse, W., Munk, M., & Reitboeck, H. J. (1988). Coherent oscillations: A mechanism of feature linking in the visual cortex? *Biol. Cybern., 60*, 121–130.

Freeman, W. J. (1975). *Mass action in the nervous system*. New York: Academic Press.

Gerstner, W., & van Hemmen, J. L. (1992). Associative memory in a network of "spiking" neurons. *Network, 3*, 139–164.

Gerstner, W., & van Hemmen, J. L. (1994). Coding and information processing in neural networks. In E. Domany, J. L. van Hemmen, K. Schulten (Eds.), *Models of neural networks II* (pp. 1–93). New York: Springer-Verlag.

Gerstner, W., Kempter, R., van Hemmen, J. L., and Wagner, H. (1996). A neuronal learning rule for sub-millisecond temporal coding. *Nature, 383*, 76–78.

Gnedenko, B. V. (1968). *The theory of probability.* (4th ed.). New York: Chelsea.

Goldberg, J. M., & Brown, P. B. (1969). Response of binaural neurons of dog superior olivary complex to dichotic tonal stimuli: Some physiological mechanisms of sound localization. *J. Neurophysiol., 32*, 613–636.

Gray, C. M., & Singer, W. (1989). Stimulus-specific neuronal oscillations in orientation columns of cat visual cortex. *Proc. Natl. Acad. Sci. USA, 86*, 1698–1702.

Ingber, L. (1982). Statistical mechanics of neocortical interactions. I. Basic formulation. *Physica, 5D*, 83–107.

Kistler, W. M., Gerstner, W., & van Hemmen, J. L. (1997). Reduction of the Hodgkin-Huxley equations to a single-variable threshold model. *Neural Comput., 9*, 1015–1045.

König, P., Engel, A. K., & Singer, W. (1995). Relation between oscillatory activity and long-range synchronization in cat visual cortex. *Proc. Natl. Acad. Sci. USA, 92*, 290–294.

König, P., Engel, A. K., & Singer, W. (1996). Integrator or coincidence detector? The role of the cortical neuron revisited. *Trends Neurosci., 19*, 130–137.

Köppl, C. (1997). Phase locking to high frequencies in the auditory nerve and cochlear nucleus magnocellularis of the barn owl, tyto alba. *J. Neurosci., 17*, 3312–3321.

Lamperti, J. (1966). *Probability.* New York: Benjamin.

Markram, H., Lübke, J., Frotscher, M., & Sakmann, B. (1997). Regulation of synaptic efficacy by coincidence of postsynaptic APs and EPSPs. *Science, 275*, 213–215.

Murthy, V. N., & Fetz, E. E. (1992). Coherent 25 to 35 Hz oscillations in the sensorimotor cortex of awake behaving monkeys. *Proc. Natl. Acad. Sci. USA, 89*, 5670–5674.

Rapp, M., Yarom, Y., & Segev, I. (1992). The impact of parallel fiber backgroud activity on the cable properties of cerebellar pulkinje cells. *Neural Comput., 4*, 518–533.

Reyes, A. D., Rubel, E. W., and Spain, W. J. (1996). In vitro analysis of optimal stimuli for phase-locking and time-delayed modulation of firing in avian nucleus laminaris neurons. *J. Neurosci., 16*, 993–1007.

Ritz, R., Gerstner, W., Fuentes, U., & van Hemmen, J. L. (1994). A biologically motivated and analytically soluble model of collective oscillations in the cortex. II. Application to binding and pattern segmentation. *Biol. Cybern., 71*, 349–358.

Ritz, R., Gerstner, W., & van Hemmen, J. L. (1994). Associative binding and segregation in a network of spiking neurons. In E. Domany, J. L. van Hemmen, K. Schulten (Eds.), *Models of neural networks II* (pp. 177–223). New York: Springe-Verlag.

Snyder, D. L., & Miller, M. I. (1991). *Random point processes in time and space.* (2nd ed.). New York: Springer-Verlag.

Softky, W. (1994). Sub-millisecond coincidence detection in active dendritic trees. *Neuroscience, 58*, 13–41.

Stemmler, M. (1996). A single spike suffices: The simplest form of stochastic resonance. *Network*, *7*, 687–716.

Theunissen, F., & Miller, J. P. (1995). Temporal encoding in nervous systems: A rigorous definition. *J. Comp. Neurosci.*, *2*, 149–162.

Troyer, T. W., and Miller, K. D. (1997). Physiological gain leads to high ISI variability in a simple model of a cortical regular spiking cell. *Neural Comput.*, *9*, 971–983.

Tsodyks, M. V., & Markram, H. (1997). The neural code between neocortical pyramidal neurons depends on neurotransmitter release probability. *Proc. Natl. Acad. Sci. USA*, *94*, 719–723.

Tuckwell, H. C. (1988). *Introduction to theoretical neurobiology: Vol. 2: Nonlinear and stochastic theories*. Cambridge: Cambridge University Press.

von der Malsburg, C., & Schneider, W. (1986). A neural cocktail-party processor. *Biol. Cybern.*, *54*, 29–40.

Wang, D., Buhmann, J., von der Malsburg, C. (1990). Pattern segmentation in associative memory. *Neural Comput.*, *2*, 94–106.

Wehr, M., & Laurent, G. (1996). Odour encoding by temporal sequences of firing in oscillating neural assemblies. *Nature*, *384*, 162–166.

Wiesenfeld, K., & Moss, F. (1995). Stochastic resonance and the benefits of noise: From ice ages to crayfish and SQUIDs. *Nature*, *373*, 33–36.

Received August 21, 1997; accepted March 16, 1998.